Study of Catalyst Coke Distribution Based on Population Balance Theory: Application to Methanol to Olefins Process

Hua Li
Dalian National Laboratory for Clean Energy, National Engineering Laboratory for MTO, Dalian Institute of Chemical Physics, Chinese Academy of Sciences, Dalian, 116023, China

Xiaoshuai Yuan and Mingbin Gao
Dalian National Laboratory for Clean Energy, National Engineering Laboratory for MTO, Dalian Institute of Chemical Physics, Chinese Academy of Sciences, Dalian, 116023, China

University of Chinese Academy of Sciences, Beijing, 100049, China

Mao Ye and Zhongmin Liu
Dalian National Laboratory for Clean Energy, National Engineering Laboratory for MTO, Dalian Institute of Chemical Physics, Chinese Academy of Sciences, Dalian, 116023, China

DOI 10.1002/aic.16518
Published online January 10, 2019 in Wiley Online Library (wileyonlinelibrary.com)

A coke distribution model of catalyst particles in three-dimensional space was developed based on population balance theory, and an analytic expression of coke distribution for zero-dimensional time-independent problem was deduced. The expression shows that the coke distribution is determined by the average catalyst residence time, coke deposition (or burning) rate, and coke distribution of catalyst inflow. The coke distribution model was further applied to the methanol to olefins (MTO) process. The critical factors influencing coke distribution in MTO process, as well as the effect of coke distribution on product selectivity, were investigated. Three scales of MTO fluidized bed reactor–regenerator systems, i.e., pilot-scale, demonstration-scale and commercial-scale with the reactor diameter of 0.261, 1.25, and 10.5 m, respectively, were simulated. The simulated results were in good agreement with the operation data. The model could be helpful in the operation optimization and reactor design. © 2018 American Institute of Chemical Engineers *AIChE J*, 65: 1149–1161, 2019
Keywords: coke distribution, population balance theory, methanol to olefins, fluidized bed, reactor-regenerator system

Introduction

Catalysts are widely used in a variety of industrial applications, and the formation of coke, which causes catalyst deactivation, is usually accompanied. For example, a number of commercial processes encounter catalyst deactivation, including steam reforming of natural gas, styrene production from ethylbenzene, catalytic cracking of heavy oil fractions, methanol to olefins (MTO) on SAPO-34, and solid acid alkylation on a Y zeolite.[1] For some processes, the catalyst particles could have a certain coke distribution. Such as for both fluid catalytic cracking (FCC) process and MTO process, the circulating fluidized bed reactor–regenerator system is adopted, where coke is deposited on the catalyst particles in the reactor and then burned off in the regenerator, as shown in Figure 1. The circulation of catalyst particles between the reactor and regenerator inevitably leads to a distribution of catalyst residence time in both the reactor and regenerator. Since coke deposition is closely related to catalyst residence time, the coke content on catalyst also demonstrates a distribution, which could be quantified by a probability density function (PDF) in mathematics. It has been found that, for some processes, coke is not only an inert substance but also it is involved in reactions, sometimes of the same type as those leading to the main products of the process.[1] Therefore, careful control of the catalyst coke distribution is required to enhance the catalytic performance in a reactor.

In order to describe the industrial processes where the coke distribution could influence the reaction performance, special attention should be paid to the calculation of the reaction rate. The reaction rate of a population of catalyst particles should be represented as $\int p(c_c)r(c_c)dc_c$, where c_c is the coke content on catalyst particles, $p(c_c)$ is the coke content PDF of the catalyst population, and $r(c_c)$ is the reaction rate with coke content c_c. Generally, the reaction rate $\int p(c_c)r(c_c)dc_c$ cannot be replaced by the rate with an average coke content, i.e., $r(\overline{c_c})$, where $\overline{c_c}$ is the average coke content of catalyst particles, i.e., $\int c_c p(c_c)dc_c$. In mathematics, only when $r(c_c)$ is a linear function of c_c, the value of $\int p(c_c)r(c_c)dc_c$ equals $r(\overline{c_c})$. However, in real commercial processes, including FCC[2] and

Additional Supporting Information may be found in the online version of this article.
Dedicated to the 70th anniversary of Dalian Institute of Chemical Physics, CAS

Correspondence concerning this article should be addressed to M. Ye at maoye@dicp.ac.cn

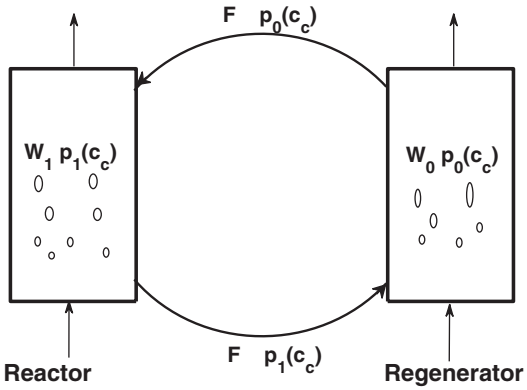

Figure 1. A reactor–regenerator system. The coke content grows in the reactor and decreases in the regenerator.

MTO,[3-5] the relation between $r(c_c)$ and c_c is highly nonlinear. Hence, the coke distribution becomes important for correctly describing the reaction behavior of a population of catalyst particles in fluidized bed reactor–regenerator system.

Age distribution approach has been traditionally used to investigate the effect of coke distribution. This approach introduces the so-called age distribution based on the perfectly mixed assumption, i.e., $E(t)=\frac{1}{\tau}\exp\left(-\frac{t}{\tau}\right)$, to predict the reaction rate by the formula $\int_0^\infty r(c_c(t))E(t)dt$, where $c_c(t)$ indicates the relation of coke content with the residence time of a particle in the fluidized bed. τ represents the average residence time of catalyst particles. In modeling of the MTO process, some researchers used the age distribution approach[6,7] to account for the influence of coke content distribution. However, the age distribution approach is an indirect method, and could not show the physical picture in a much clearer way. Most of the interested properties in the MTO process, such as product selectivity, methanol conversion, and average coke content, require the direct information of the coke distribution, i.e., $p(c_c)$. It is necessary to develop a direct method, i.e., coke distribution approach, to obtain coke distribution. The key of age distribution approach is how to get the function $E(t)$, and how to map residence time to coke content of catalyst particles. Under the perfectly mixed assumption, the expression of $E(t)$ could be analytically derived, and the map function could be easily obtained when the coke deposition rate has simple relation with coke content. In this case, the age distribution approach could give the same results as coke distribution approach for zero-dimensional (0D) time-independent problem when the inflow catalyst particles have a single coke content. However, for space-dependent or time-dependent problem, or when the inflow catalyst particles have a certain coke distribution, the derivation of $E(t)$ or the mapping of t to c_c is extremely hard, if not impossible. In this connection, the coke distribution approach is clearly superior over the age distribution approach and could provide a direct yet simple way to investigate coke distribution in real MTO reactor.

The population balance theory or mass balance theory provides a powerful tool to obtain the PDF of coke distribution. As early as 1964, Hulburt and Katz[8] separated the coordinates of a particle into two parts—a set of external coordinates which specify the location of the particle and a set of internal coordinates that specify the particle size and other aspects of the particles quality as may be relevant; then they derived the (time-dependent three-dimension [3D]) population balance equation for particle size according to the conservation of number density of particles in the phase space. In 1968, Levenspiel et al.[9] developed the general equations in terms of mass balances to relate the particle size distributions with flow rates of feeds and outflow streams in fluidized beds. The equations[9], which are essentially based on the 0D particle population and independent of time, have analytical solutions if special boundary conditions are applied. All these works well inspired us to develop our coke distribution equation. Here we focus on the particle weight (catalyst plus coke), and the aim of the current work is to obtain a clearer and simpler equation of the coke distribution of catalyst particles, and then apply it to MTO process.

The MTO process provides an alternative approach to produce light olefins from nonoil resources, and has become a subject of intense researches spanning catalyst synthesis, reaction mechanism, reaction kinetics, process development, and reactor scale-up.[10,11] In August 2010, a commercial unit (600 kt/a of ethylene and propylene production), based on the MTO technology (DMTO) developed by Dalian Institute of Chemical Physics (DICP), was successfully started up in Shenhua's Baotou coal-to-olefins plant in north China.[12] In the open literature, various reactor and kinetic models, as well as computational fluid dynamics (CFD) simulations, have been proposed for the MTO process.[3-7,13-16] Only a few took effect of coke distribution into account using age distribution approach.[6,7]

In this article, a (time-dependent 3D) coke distribution model of catalyst particles based upon the population balance theory was established, and an analytical formula of 0D time-independent coke distribution was further obtained. Three scales of reactor–regenerator systems of MTO process, i.e., pilot-scale, demonstration-scale, and commercial-scale with reactor diameters of 0.261, 1.25, and 10.5 m, respectively, were simulated. All simulated results were compared with experimental values. Here, a MTO kinetic model recently developed by our group[5] was applied to derive the kinetic parameters, and the generic fluidized-bed reactor (GFBR) model,[17] which spans bubbling, turbulent, and fast fluidization regimes, was used to describe the flow state of the fluidized bed.

Coke Distribution Model

In this section, the coke distribution model is derived based on the conservation of mass of catalyst particles.

Model

In order to describe the motion of a population of catalyst particles, we first define the phase coordinates of catalyst particles. The coordinates of a particle could be separated into two parts: a set of external rectangular Cartesian coordinates, i.e., $\vec{x}$ or x_i (i = 1,2,3; in m), which specify the spacial location of the particle; and an internal coordinate, i.e., coke content c_c (in *dimensionless*), which specify the mass ratio of the coke to the particle. Then the corresponding velocities of the particle could be obtained.

$$\frac{dx_i}{dt}=v_i\left(\vec{x},t\right) \tag{1}$$

$$\frac{dc_c}{dt}=R(c_c) \tag{2}$$

Here $v_i\left(\vec{x},t\right)$ (in $\frac{\mathrm{m}}{\mathrm{s}}$) represents spacial velocities of the particle, and $R(c_c)$ (in $\frac{1}{\mathrm{s}}$) represents the coke deposition rate or coke burning rate, and t (in s) is time.

For a population of catalyst particles that occupy a volume $V(t)$, including the internal coordinate c_c, the mass is conserved, which could be expressed as following:

$$\frac{d}{dt}\int_{V(t)} \rho_{cat}(\vec{x},t)p(\vec{x},c_c,t)dx_1dx_2dx_3dc_c = 0 \tag{3}$$

where $\rho_{cat}(\vec{x},t)$ (in $\frac{kg}{m^3}$) represents the time-dependent mass density of catalyst particles at location $\vec{x}$ and time t, and $p(\vec{x},c_c,t)$ (in *dimensionless*) is the PDF of coke content. Here $\rho_{cat}(\vec{x},t)$ refers to the mass density of net catalyst particles, not including the coke deposited on them. The function $p(\vec{x},c_c,t)$ possesses a property that

$$\int p(\vec{x},c_c,t)dc_c = 1. \tag{4}$$

From Eq. 3, the following relation could be derived

$$\begin{aligned}\frac{\partial \rho_{cat}(\vec{x},t)p(\vec{x},c_c,t)}{\partial t} &+ \nabla\cdot\left[\vec{v}(\vec{x},t)\rho_{cat}(\vec{x},t)p(\vec{x},c_c,t)\right] \\ &+ \frac{\partial\left[R(c_c)\rho_{cat}(\vec{x},t)p(\vec{x},c_c,t)\right]}{\partial c_c} = 0.\end{aligned} \tag{5}$$

Equation 5 is a time-dependent 3D partial differential equation (PDE) for the coke distribution model based on the catalyst mass density. This equation could be solved by coupling with other conservation equations, which may provide the information of velocity and density of catalyst particles.

Time-dependent problem

In the simulations of a catalytic process, different assumptions, such as the completely mixing and plug flow, are commonly used to simplify the reactor model. The coke distribution equation, i.e., Eq. 5, could be also simplified based on these assumptions. In this subsection, the 0D and one-dimensional (1D) time-dependent coke distribution models are obtained.

0D Coke Distribution Model. Fluidized bed reactor could be viewed as 0D system, if catalyst particles in the bed are assumed to be perfectly mixed. For such system, the simplified form of Eq. 5 could be written as

$$\begin{aligned}\frac{\partial[W(t)p(c_c,t)]}{\partial t} &+ F_{out}(t)p(c_c,t) - F_{in}(t)p_{in}(c_c,t) \\ &+ W(t)\frac{\partial[R(c_c)p(c_c,t)]}{\partial c_c} = 0,\end{aligned} \tag{6}$$

where $W(t)$ (in kg) is the catalyst inventory in the bed, $F_{out}(t)$ (in $\frac{kg}{s}$) is the outflow flux of catalyst particles, $F_{in}(t)$ (in $\frac{kg}{s}$) is the inflow flux of catalyst particles, and $p_{in}(c_c, t)$ (in *dimensionless*) is the PDF of inflow catalyst particles. The three quantities $W(t)$, $F_{out}(t)$, and $F_{in}(t)$ only refer to the mass of the catalyst particles, do not include any coke deposited on them. Assuming that the catalyst inventory, outflow flux, and inflow flux are independent of time, and further $F_{in}(t) = F_{out}(t)$ (thus the two fluxes could be abbreviated by F, in $\frac{kg}{s}$), we could obtain

$$\frac{\partial p(c_c,t)}{\partial t} + \frac{\partial[R(c_c)p(c_c,t)]}{\partial c_c} = \frac{1}{\tau}[p_{in}(c_c,t) - p(c_c,t)], \tag{7}$$

where τ (in s) is the average residence time of catalyst particles, i.e., $\tau = \frac{W}{F}$. If there is no catalyst flux for the bed, i.e., $F \to 0$ or $\tau \to \infty$, the Eq. 7 could be written as

$$\frac{\partial p(c_c,t)}{\partial t} + \frac{\partial[R(c_c)p(c_c,t)]}{\partial c_c} = 0. \tag{8}$$

The above equation could also be applied to describe the coke distribution of catalyst particles in a small region of a fixed bed reactor, since all catalyst particles in the bed are fixed, i.e., $\vec{v} = 0$.

1D Coke Distribution Model. For a plug-flow reactor, the catalyst particles could be assumed to be transported along the reactor axis (z-axis) with constant velocity, i.e., v_z (in $\frac{m}{s}$), and constant catalyst density. Then the Eq. 5 could be simplified as

$$\frac{\partial p(z,c_c,t)}{\partial t} + v_z\frac{\partial p(z,c_c,t)}{\partial z} + \frac{\partial[R(c_c)p(z,c_c,t)]}{\partial c_c} = 0. \tag{9}$$

Time-independent problem

In this section, 0D time-independent coke distribution equations are first obtained, and nonzero-dimensional time-independent coke distribution equations are then derived.

0D Coke Distribution Equations. The time-independent equation could be obtained from Eq. 7 as follows

$$\frac{d[R(c_c)p(c_c)]}{dc_c} = \frac{1}{\tau}[p_{in}(c_c) - p(c_c)]. \tag{10}$$

From Eq. 10, we could derive the analytic solution of $p(c_c)$ for $R(c_c) > 0$ (see Supporting Information Appendix A).

$$p(c_c) = \frac{1}{\tau R(c_c)}\int_{c_c^{min}}^{c_c} p_{in}(c_c^{ini})e^{-\int_{c_c^{ini}}^{c_c}\frac{1}{\tau R(s)}ds}dc_c^{ini} \tag{11}$$

Here, c_c^{min} (in *dimensionless*) is the minimum coke content of inflow catalyst particles. Similarly, we could obtain the expression of $p(c_c)$ for $R(c_c) < 0$ as follows

$$p(c_c) = \frac{1}{-\tau R(c_c)}\int_{c_c}^{c_c^{max}} p_{in}(c_c^{ini})e^{-\int_{c_c}^{c_c^{ini}}\frac{1}{-\tau R(s)}ds}dc_c^{ini}, \tag{12}$$

where c_c^{max} (in *dimensionless*) is the maximum coke content of inflow catalyst particles.

If the inflow catalyst particles have only a single coke content, i.e., c_c^0, which represents that $p_{in}(c_c)$ is a delta function, i.e., $p_{in}(c_c) = \delta(c_c - c_c^0)$, the above two equations (Eqs. 11, 12) could be simplified respectively as

$$p(c_c) = \frac{1}{\tau R(c_c)}e^{-\int_{c_c^0}^{c_c}\frac{1}{\tau R(s)}ds} \tag{13}$$

$$p(c_c) = \frac{1}{-\tau R(c_c)}e^{-\int_{c_c}^{c_c^0}\frac{1}{-\tau R(s)}ds}. \tag{14}$$

It is interesting that the PDF of coke distribution is identical to the residence time distribution, i.e., $\frac{1}{\tau}e^{-\frac{t}{\tau}}$, by setting $R(c_c) = 1$ and $c_c^0 = 0$ in Eq. 13. If the relation of $R(c_c)$ with c_c is known, an explicit expression of $p(c_c)$ could be obtained from Eqs. 13, 14.

Nonzero Dimensional Coke Distribution Equations. The equation of nonzero-dimensional coke distribution can be obtained from the 0D time-independent expression. Logically, if we could get the PDF in an arbitrary cell in nonzero-dimensional space, the PDFs of the whole space could be obtained.

Now, we focus on an arbitrary cell, denoted as P, in the reactor. Catalyst particles in the cell are assumed to be perfectly mixed. For convenience, we define the catalyst inflow

through each face f of cell P as F^f (kg/s), the PDF of the neighbor cell which connected by face f as $p^{N_f}(c_c)$ (*dimensionless*), and the mass of catalyst particles in the cell as W^P (kg). Note that the inflow term F^f which represents the flux leaving from the neighbor cell is different with the net flux through the face f. Then we could obtain the total mass of inflow or outflow of cell P, i.e., $F^P = \sum_f F^f$ (its unit is $\frac{\text{kg}}{\text{s}}$), and the average residence time of the particles in the cell, i.e., $\tau^P = \frac{W^P}{F^P}$ (its unit is s). The PDF of cell P for $R(c_c) > 0$ could be

$$p^P(c_c) = \frac{1}{\tau^P R(c_c)} \int_{c_c^{\min}}^{c_c} e^{-\int_{c_c^{\text{ini}}}^{cc} \frac{1}{\tau R(s)} ds} \sum_f \left(\frac{F^f}{F^P} p^{N_f}\left(c_c^{\text{ini}}\right) \right) dc_c^{\text{ini}}. \quad (15)$$

For $R(c_c) < 0$, the PDF of cell P is

$$p^P(c_c) = \frac{1}{-\tau^P R(c_c)} \int_{c_c}^{c_c^{\max}} e^{-\int_{c_c}^{c_c^{\text{ini}}} \frac{1}{-\tau R(s)} \mathrm{d}s} \sum_f \left(\frac{F^f}{F^P} p^{N_f}\left(c_c^{\text{ini}}\right) \right) dc_c^{\text{ini}}. \quad (16)$$

The derivation in this section can be viewed as an extension of the derivation of section *0D Coke Distribution Equations*. By comparing Eq. 11 and Eq. 15, we could find that the two situations are physically the same.

Application to MTO Process

In this section, the 0D time-independent model was applied to the reactor–regenerator system of the MTO process, where coke is deposited in the fluidized bed reactor [$R(c_c) > 0$] and burned off in the fluidized bed regenerator [$R(c_c) < 0$]. The catalyst particles in the reactor and regenerator are assumed to be perfectly mixed.

The simplified scheme of a typical reactor–regenerator system is shown in Figure 1. In Figure 1, W_1 (in kg) and W_0 (in kg) denote the catalyst inventory in the reactor and regenerator, respectively, and F (in $\frac{\text{kg}}{\text{s}}$) represents the catalyst circulation rate between the reactor and regenerator. At steady-state, the catalyst circulation rate is equal to the rate of catalyst inflow and/or outflow of each bed. The three quantities W_1, W_0, and F only refer to mass of the catalyst particles, do not including any coke that has been deposited on them. $p_1(c_c)$ (in *dimensionless*) indicates the PDF of coke content on catalyst particles of the reactor, while $p_0(c_c)$ (in *dimensionless*) indicates that of regenerator.

Coke distribution

The PDF of the reactor is highly related to the coke deposition rate $R_1(c_c)$. Based on the kinetics recently proposed by Yuan et al.,[5] the coke deposition rate could be expressed as

$$R_1(c_c) = k_d s(c_c) \quad (17)$$

where

$$s(c_c) = c_c^{\max} - c_c \quad (18)$$

$$k_d = k_8 \hat{\rho}_{\text{MeOH}}^{0.3} + k_9 \hat{\rho}_{\text{C}_2\text{H}_4}^{0.3} + k_{10} \hat{\rho}_{\text{C}_3\text{H}_6}^{0.3} + k_{11} \hat{\rho}_{\text{C}_4\text{H}_8}^{0.3} + k_{12} \hat{\rho}_{\text{C}_{5+}}^{0.3} \quad (19)$$

$s(c_c)$ (in *dimensionless*) represents the content of the active sites of the catalyst particle. Here $c_c^{\max}$ (in *dimensionless*) is the maximum coke content of the catalyst particle. k_d (in $\frac{1}{\text{s}}$) is the deposition rate constant, which is related to the densities of methanol and olefins, $\hat{\rho}_i$ (in $\frac{\text{kg}}{\text{m}^3}$) is the density of species i which is calculated based on the voidage volume.[5]

In this work, the used coke deposition rate was obtained via a MTO reaction kinetic model recently developed in our group,[5] in which the MTO reaction over SAPO-34 catalyst is assumed to follow the advanced dual-cycle reaction mechanism. In this model, both the olefins-based cycle and aromatics-based cycle are denoted as virtual species, where the former mainly accounts for the production of higher olefins and the latter for lower olefins. The kinetic parameters including coke deposition rate were derived by fitting experimental data from laboratory scale fluidized bed reactor with commercial DMTO catalyst.

From Eqs. 11, 17, we could obtain

$$p_1(c_c) = \int_{c_c^{\min}}^{c_c} \frac{1}{\tau_1 k_d \left(c_c^{\max} - c_c^{\text{ini}}\right)} \left(\frac{c_c^{\max} - c_c}{c_c^{\max} - c_c^{\text{ini}}} \right)^{\frac{1}{\tau_1 k_d} - 1} p_0\left(c_c^{\text{ini}}\right) dc_c^{\text{ini}} \quad (20)$$

Then, we could have the average coke content in the reactor.

$$\overline{c_{c1}} = \int_{c_c^{\min}}^{c_c^{\max}} c_c p_1(c_c) dc_c = \frac{\tau_1 k_d}{1 + \tau_1 k_d} c_c^{\max} + \frac{1}{1 + \tau_1 k_d} \int_{c_c^{\min}}^{c_c^{\max}} c_c^{\text{ini}} p_0\left(c_c^{\text{ini}}\right) dc_c^{\text{ini}} \quad (21)$$

When the catalyst inflow of the reactor only has a narrow cut of coke content, where the coke content is around c_c^0, which implied that the $p_0(c_c)$ could be approximated by the function $\delta\left(c_c - c_c^0\right)$, the Eq. 20 could be simplified as

$$p_1(c_c) = \frac{1}{\tau_1 k_d \left(c_c^{\max} - c_c^0\right)} \left(\frac{c_c^{\max} - c_c}{c_c^{\max} - c_c^0} \right)^{\frac{1}{\tau_1 k_d} - 1} \quad (22)$$

And, the Eq. 21 could be written as

$$\overline{c_{c1}} = \frac{\tau_1 k_d}{1 + \tau_1 k_d} c_c^{\max} + \frac{1}{1 + \tau_1 k_d} c_c^0. \quad (23)$$

The burning rate R_0 in the regenerator could be expressed as

$$R_0(c_c) = -k_b c_c^m \quad (24)$$

where k_b (in $\frac{1}{\text{s}}$) is the burning rate constant, and m (in *dimensionless*) is the order of reaction. Based on our previous experimental results, we found that m is approximately 1, and k_b could be expressed as a linear function of the pressure of O_2, i.e., $k_b = k_{O_2} p_{O_2}$, where p_{O_2} (Pa) is the pressure of O_2 and k_{O_2} ($\frac{1}{\text{Pas}}$) is rate parameter. By setting $m = 1$, we could derive the expression of p_0 from Eqs. 12, 24 as following

$$p_0(c_c) = \int_{c_c}^{c_c^{\max}} \frac{1}{\tau_0 k_b c_c^{\text{ini}}} \left(\frac{c_c}{c_c^{\text{ini}}} \right)^{\frac{1}{\tau_0 k_b} - 1} p_1\left(c_c^{\text{ini}}\right) dc_c^{\text{ini}} \quad (25)$$

Now we could have the average coke content in the regenerator.

$$\overline{c_{c0}} = \int_{c_c^{\min}}^{c_c^{\max}} c_c p_0(c_c) dc_c = \frac{1}{1 + \tau_0 k_b} \int_{c_c^{\min}}^{c_c^{\max}} c_c^{\text{ini}} \left[1 - \left(\frac{c_c^{\min}}{c_c^{\text{ini}}} \right)^{\frac{1}{\tau_0 k_b} + 1} \right] p_1\left(c_c^{\text{ini}}\right) dc_c^{\text{ini}} \quad (26)$$

Here, c_c^{min} equals zero, and then we could further obtain

$$\overline{c_{c0}} = \frac{1}{1+\tau_0 k_b} \int_{c_c^{min}=0}^{c_c^{max}} c_c^{ini} p_1\left(c_c^{ini}\right) dc_c^{ini} \tag{27}$$

In this subsection, we introduced the PDFs of coke content and the average coke content in both reactor and regenerator in MTO process. We could find that two constants, i.e., k_d and k_b, play an important role in these calculations. The specific scheme for calculating k_d and k_b is introduced in next subsection.

Reactor model

The hydrodynamics of both reactor and regenerator is described by the GFBR model.[17] The fluidized beds, according to the GFBR model, are divided into two parts, i.e., freeboard and dense bed, as shown in Figure 2. The dense bed is further divided into two parts: the dilute phase/region using the descriptor "low-density" (L) phase, and the dense phase/region using the descriptor "high-density" (H) phase. The L-phase represents the bubble phase at low velocity and the core region at high velocity, while the H-phase represents dense or emulsion phase at low velocity and the outer annular region at high velocity.

Then the control equations of steady-state for L-phase and H-phase in a fluidized bed could be represented as[17]

$$\psi_L u_L \frac{dC_{iL}}{dz} = \psi_L D_L \frac{d^2 C_{iL}}{dz^2} - k_{LH} a_I \psi_L (C_{iL} - C_{iH}) + \psi_L \overline{r_{iL}}, \tag{28}$$

$$\psi_H u_H \frac{dC_{iH}}{dz} = \psi_H D_H \frac{d^2 C_{iH}}{dz^2} - k_{LH} a_I \psi_L (C_{iH} - C_{iL}) + \psi_H \overline{r_{iH}}, \tag{29}$$

and the control equation for freeboard could be represented as

$$u_f \frac{dC_{if}}{dz_f} = D_f \frac{d^2 C_{if}}{dz_f^2} + \overline{r_{if}}. \tag{30}$$

Here, the three equations are 1D differential equations, which neglect the changes of the concentrations along the radial direction. In these equations, ψ_S (in *dimensionless*) represents the S-phase volume fraction, and u_S (in $\frac{m}{s}$) indicates the superficial velocity of gas of S-phase, D_S (in $\frac{m^2}{s}$) means the axial gas dispersion coefficient of S-phase, C_{iS} (in $\frac{kmol}{m^3}$) is the concentration of species i of S-phase, and $\overline{r_{iS}}$ (in $\frac{kmol}{m^3 s}$) is the average reaction rate due to coke distribution of S-phase. Here, the subscript S denotes L, H, or f. Hereafter, we will neglect the subscript L, H, and f for simplicity. k_{LH} (in $\frac{m}{s}$) represents gas interchange coefficient between L and H phases, and a_I (in $\frac{1}{m}$) represents interphase transfer surface per unit volume of gas in low-density phase.

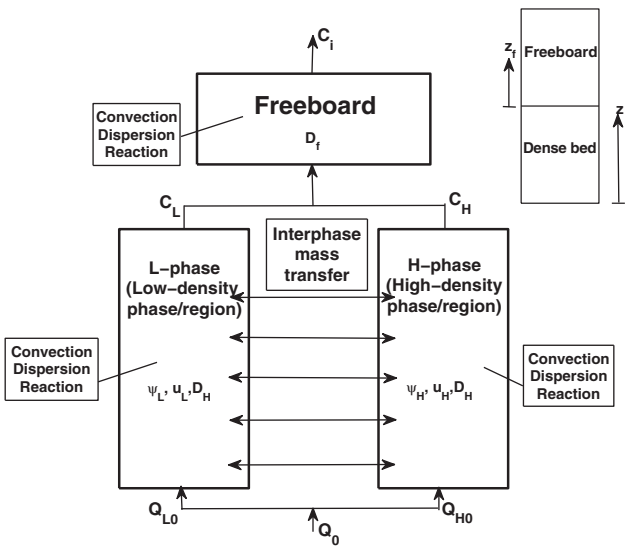

Figure 2. A sketch of GFBR model.[17]

The parameters ψ, u, D, as well as k_{LH} and a_I, could be predicted by the GFBR model (see reference [17] for details). Therefore, we should focus our attention on the term $\overline{r_i}$, whose expression could be written as

$$\overline{r_i} = \int_{c_c^{min}}^{c_c^{max}} r_i(c_c) p_1(c_c) dc_c. \tag{31}$$

The rate of species i, i.e., $r_i(c_c)$ (in $\frac{kmol}{m^3 s}$), can be expressed by linear sum of rates of reaction equations

$$r_i(c_c) = \sum_j c_{ji} \mathscr{R}_j(c_c) \epsilon / M_i \tag{32}$$

where c_{ji} (in *dimensionless*) is coefficient of reaction equation, ϵ (in *dimensionless*) is the voidage of the current phase, and M_i (in $\frac{kg}{kmol}$) is molar mass of species *i*. The rate of reaction equation j, i.e., $\mathscr{R}_j(c_c)$ (in $\frac{kg}{m^3 s}$), according to its relation with coke content c_c (see the reference [5] for details), could be written in three forms

$$\mathscr{R}_j(c_c) = \begin{cases} k_j^e s(c_c) \\ k_j^e s(c_c) \phi(c_c) \\ k_j^e c_c \phi(c_c) \end{cases} \tag{33}$$

where $s(c_c) = c_c^{max} - c_c$ (as defined in Eq. 18), and k_j^e (in $\frac{kg}{m^3 s}$) is effective rate parameter of equation j, which incorporate the effect of densities of reactants and catalyst particles. $\phi(c_c)$ (in *dimensionless*) is deactivation function of catalyst

$$\phi(c_c) = \exp\left\{ -\left[\left(\frac{c_c^{max} - c_c^{cri}}{c_c^{max} - c_c} \right)^5 - \left(\frac{c_c^{max} - c_c^{cri}}{c_c^{max}} \right)^5 \right] \right\} \tag{34}$$

where c_c^{cri} (in *dimensionless*) is a parameter of activation, which could be calculated by the relation $c_c^{cri} = 0.10 - 0.021 \ln WHSV$. WHSV (in $\frac{kg\ MeOH}{kg\ Cat\ h}$) is the ratio of the methanol influx of the reactor to the mass of catalyst particles in the reactor.

From Eqs. 31–33, we could find that the effect of coke distribution on the reaction rates of species is embodied in three terms, i.e., $\int_{c_c^{min}}^{c_c^{max}} s(c_c) p_1(c_c) dc_c$, $\int_{c_c^{min}}^{c_c^{max}} s(c_c) \phi(c_c) p_1(c_c) dc_c$, and $\int_{c_c^{min}}^{c_c^{max}} c_c \phi(c_c) p_1(c_c) dc_c$. For convenience, we denote them by symbols $\overline{s_1}$, $\overline{(s\phi)_1}$, and $\overline{(c_c\phi)_1}$, respectively. Based on the relation $c_c^{max} = \overline{c_{c1}} + \overline{s_1}$, we could get the expression of $\overline{s_1}$ from Eq. 21

$$\overline{s_1} = \frac{1}{1+\tau_1 k_d} c_c^{max} - \frac{1}{1+\tau_1 k_d} \int_{c_c^{min}}^{c_c^{max}} c_c^{ini} p_0\left(c_c^{ini}\right) dc_c^{ini} \tag{35}$$

And the expressions of $\overline{(s\phi)_1}$ and $\overline{(c_c\phi)_1}$ are given in Supporting Information Appendix B.

It is obvious that we cannot, based on the kinetics proposed by Yuan et al.,[5] replace the average rate $\int r(c_c)p_1(c_c)dc_c$ by $r(\overline{c_c})$.

The whole system could be solved iteratively. A special parameter is k_d, which should be updated after solving three control equations. From Eqs. 28–30, we could get the species concentrations, as well as the corresponding rate of coke deposition, along with the height of the reactor. This rate of coke deposition, which changes with the height of the reactor, is the local deposition rate dependent upon the local densities of species and catalyst particles. Since the catalyst particles are assumed to be perfectly mixed in the reactor, the value of $R_1(c_c)$ is in fact a mass averaged value of these local rates of coke deposition. Then, based on Eq. 17, the k_d could be obtained by equation

$$k_d = R_1(c_c)\overline{s_1}. \tag{36}$$

Subsequently, the value of $\overline{s_1}$, $\overline{(s\phi)_1}$, and $\overline{(c_c\phi)_1}$ could be updated with new k_d. Then we return to solve the control equations, and the procedure is then iterated.

Results and Discussion

Time-independent coke distribution

In this section, we investigated some properties of time-independent coke distribution for the reaction processes in which the coke deposition (burning) rate is linearly dependent on the coke content, such as MTO process based on our proposed kinetics.[5]

0D Coke Distribution. From Eq. 11, it could be found that the average catalyst residence time, coke deposition rate and coke distribution of catalyst inflow determine the coke distribution of the reactor. If the deposition (burning) rate is a linear function of coke content, the first two factors, could be considered together as a single factor, which can be represented by a dimensionless number, i.e., $\tau_1 k_d$ (see Eq. 20). Here we introduce the Dahmkohler number $\Gamma_1 \equiv \tau_1 k_d$ for convenience. If the catalyst inflow has a single coke content, the dependence of coke distribution upon Γ_1 is given by Eq. 22. Figure 3 shows the change of coke distribution with Γ_1, where $c_c^{max} = 0.11$ and $c_c^0 = 0$. It reveals that, if $\Gamma_1 = 1$, the PDF of coke

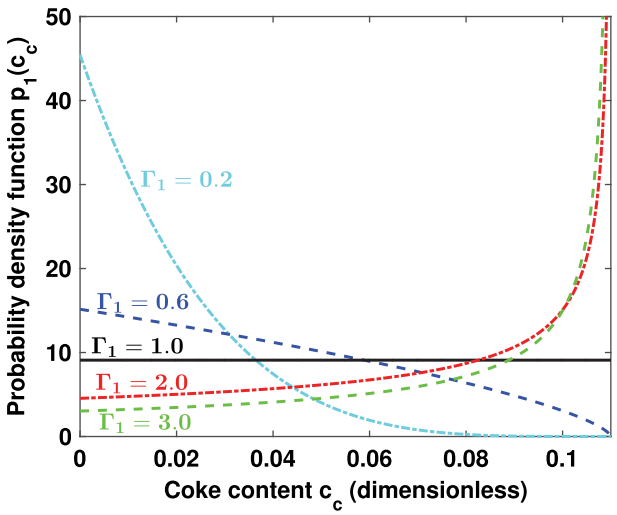

Figure 3. The relation of coke distributions with Γ_1 ($\Gamma_1 \equiv \tau_1 k_d$, $c_c^{max} = 0.11$, $c_c^0 = 0$).
[Color figure can be viewed at wileyonlinelibrary.com]

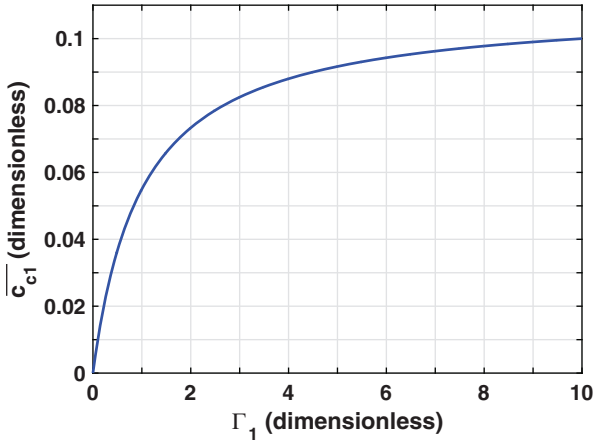

Figure 4. The average coke content as a function of Γ_1 ($\Gamma_1 \equiv \tau_1 k_d$, $c_c^{max} = 0.11$, $c_c^0 = 0$).
[Color figure can be viewed at wileyonlinelibrary.com]

content is constant, which means a uniform distribution of coke content; if $\Gamma_1 < 1$, the PDF is a monotonically decreasing function, which shows the superiority of low coke content; if $\Gamma_1 > 1$, the PDF is a monotonically increasing function that reflects the superiority of high coke content. It is critical to choose an appropriate coke distribution of the reactor by setting a suitable value of Γ_1. It could further be found that Γ_1 is highly related to the average coke content $\overline{c_{c1}}$, as shown in Eq. 21, 23. These two equations are identical in nature, if we regard $\int_{c_c^{min}}^{c_c^{max}} c_c^{ini} p_0(c_c^{ini}) dc_c^{ini}$ as $\overline{c_{c0}}$. Figure 4 shows a monotonically increasing function of $\overline{c_{c1}}$ in regard to Γ_1. More importantly, we could estimate Γ_1 from the value of $\overline{c_{c1}}$ via the following relation established based on experiments.

$$\Gamma_1 = \frac{\overline{c_{c1}} - \overline{c_{c0}}}{c_c^{max} - \overline{c_{c1}}} \tag{37}$$

It also implies that, if we want to keep a certain average coke content in the reactor, we could choose a suitable Γ_1 based on Eq. 37 for the reactor. It is similar for regenerator, see Eq. 27.

Another factor that could affect the coke distribution of the reactor is coke distribution of catalyst inflow, i.e., $p_0(c_c)$. This could be investigated by observing the changes of PDFs in a virtual circulating process of reactor–regenerator system, which also means a numerical iteration process. As can be seen in Figures 5 and 6, the results after two iterations are very close to that for 3 and 10 iterations, which suggests that the final steady-state of both reactor and regenerator could be quickly reached after two numerical iterations at present study. During the circulation, the average coke contents of both beds are fixed with given values. Figure 5 shows the coke distributions of both reactor and regenerator, where the average coke contents are fixed with 5.28% and 1.43%, respectively (here $c_c^{max} = 11.7\%$, $c_c^{min} = 0.0\%$). We could obtain $\Gamma_1 = 0.60$ from Eq. 37. The coke distribution of the regenerator is first assumed to be $\delta(c_c - 0.0143)$, that is to say, all the catalyst particles in the regenerator has a single coke content of 1.43%. Such distribution of $p_0(c_c)$ is displayed in Figure 5 by a blue dashed line. At this coke distribution of catalyst inflow, we could obtain the coke distribution of the reactor, i.e., $p_1(c_c)$, from Eq. 20, which is shown in Figure 5 also by a blue dashed line. This $p_1(c_c)$ then becomes the coke distribution of the

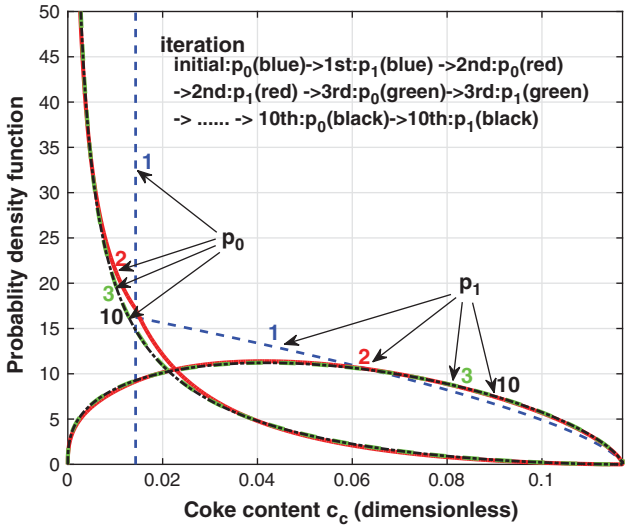

Figure 5. The coke distributions of reactor–regenerator system.

The average coke contents of the reactor and regenerator are fixed with 5.28% and 1.43%, respectively ($c_c^{max} = 0.117$). [Color figure can be viewed at wileyonlinelibrary.com]

inflow of the regenerator, and we could obtain new $p_0(c_c)$ as shown in Figure 5 by a red solid line, which now shows a certain distribution and becomes different to its initial setting (a single coke content). At this $p_0(c_c)$ distribution, we could obtain new $p_1(c_c)$, as shown in Figure 5 by a red solid line, which also is different to the distribution in previous iteration. The $p_1(c_c)$ in the previous iteration, shown by a blue dashed line, is a monotonically decreasing function, while the new one has a maximum. For a further iteration, the profiles of new PDFs of both beds, shown in green dash-dot lines, are similar to the PDFs before this iteration, which means the PDFs are close to convergence. Another situation where the coke content in the reactor is fixed with 7.80% is also considered. The corresponding Γ_1 is 1.63 based on Eq. 37. The simulation of the circulating process is shown in Figure 6. Different with our previous example, the convergent PDF of

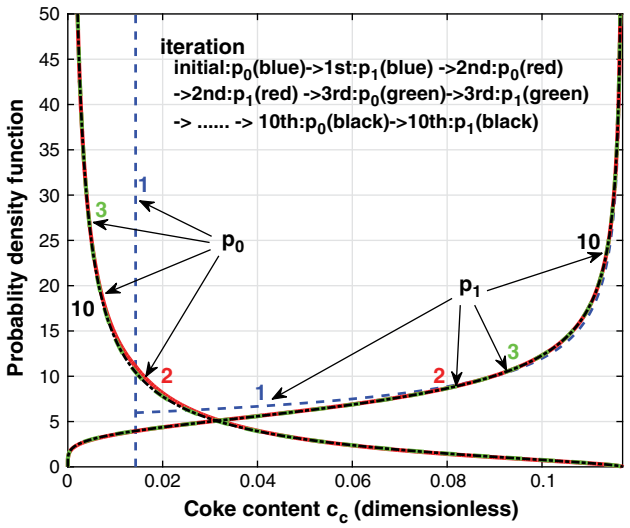

Figure 6. The coke distributions of reactor–regenerator system.

The average coke contents of the reactor and regenerator are fixed with 7.80% and 1.43%, respectively ($c_c^{max} = 0.117$). [Color figure can be viewed at wileyonlinelibrary.com]

current $p_1(c_c)$ is a monotonically increasing function. It seems that $\Gamma_1 = 1$ also becomes a critical point for $p_1(c_c)$, as shown in Figures 5 and 6, where Γ_1 equals 0.60 and 1.63, respectively.

Nonzero-Dimensional Coke Distribution. For a nonzero-dimensional problem, the coke distribution could be influenced by back mixing flow of catalyst particles. The coke distribution equations of such problem are given in section *Nonzero-Dimensional Coke Distribution Equations.* In this section, the effect of the back mixing of catalyst particles was demonstrated by a simplified modeling reactor (Figure 7).

The reactor here is divided into two connected fluidized beds, as shown in Figure 7. Each bed is assumed to have same catalyst inventory of $\frac{W_1}{2}$, and the catalyst particles in each bed are assumed to be perfectly mixed. The coke distributions of two beds are represented by $p_1^F(c_c)$ (dimensionless) and $p_1^S(c_c)$ (dimensionless), respectively. The back mixing flow of catalyst particles between two beds is denoted by F_{bm} (in $\frac{kg}{s}$).

From Eqs. 15, 20, we could obtain the coke distributions of two beds (see Supporting Information Appendix C for details).

$$p_1^F(c_c) = \int_{c_c^{min}}^{c_c} \frac{1}{\Gamma_1^F\left(c_c^{max} - c_c^{ini}\right)} \left(\frac{c_c^{max} - c_c}{c_c^{max} - c_c^{ini}}\right)^{\frac{1}{\Gamma_1^F}-1} p_0^{F,e}\left(c_c^{ini}\right) dc_c^{ini} \tag{38}$$

$$p_1^S(c_c) = \int_{c_c^{min}}^{c_c} \frac{1}{\Gamma_1^S\left(c_c^{max} - c_c^{ini}\right)} \left(\frac{c_c^{max} - c_c}{c_c^{max} - c_c^{ini}}\right)^{\frac{1}{\Gamma_1^S}-1} p_0^{S,e}\left(c_c^{ini}\right) dc_c^{ini} \tag{39}$$

where

$$p_0^{F,e}(c_c) = \frac{\Gamma_{1,bm}}{\Gamma_1 + \Gamma_{1,bm}} p_0(c_c) + \frac{\Gamma_1}{\Gamma_1 + \Gamma_{1,bm}} p_1^S(c_c) \tag{40}$$

$$p_0^{S,e}(c_c) = p_1^F(c_c) \tag{41}$$

$$\Gamma_1^F = \Gamma_1^S = \frac{1}{2} \frac{\Gamma_1 \Gamma_{1,bm}}{\Gamma_1 + \Gamma_{1,bm}} \tag{42}$$

Here $\Gamma_{1,bm} \equiv \frac{W_1}{F_{bm}} k_d$.

From Eqs. 38–42, it could find that Γ_1, $\Gamma_{1,\,bm}$, and $p_0(c_c)$ determine the coke distributions of the reactor when the catalyst inventory and k_d are identical for two beds in the reactor. If $\Gamma_{1,\,bm} \to 0+$, i.e., $F_{bm} \to +\infty$, all catalyst particles in two beds of the reactor will be perfectly mixed, then the problem

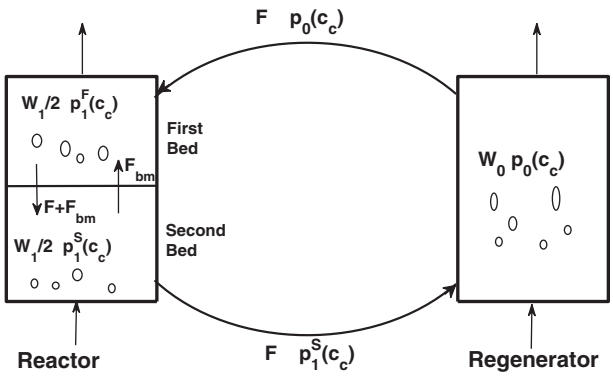

Figure 7. A reactor–regenerator system.

The reactor is divided into two connected fluidized beds (the first bed and second bed).

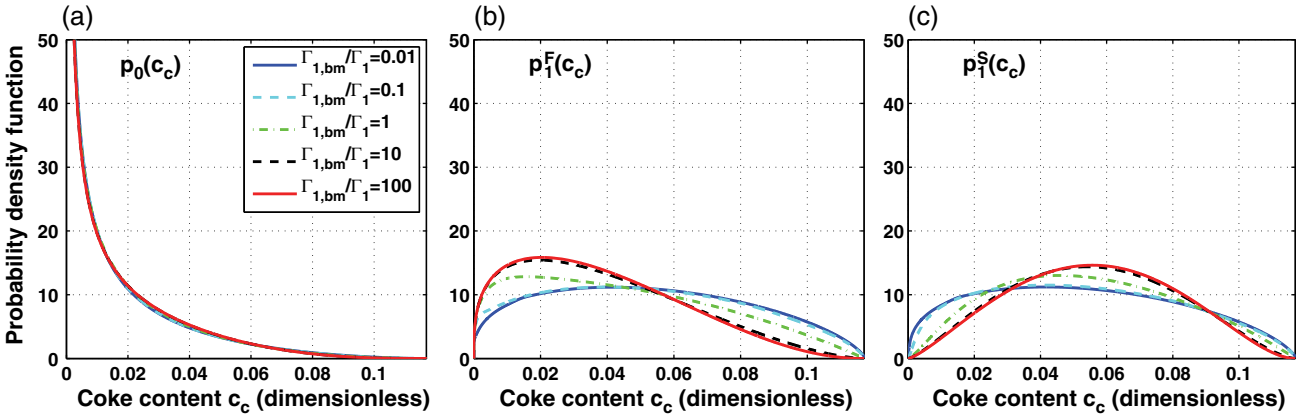

Figure 8. The coke distributions of reactor–regenerator system. (a) $p_0(c_c)$, (b) $p_1^F(c_c)$, and (c) $p_1^S(c_c)$.

The average coke content of the regenerator is fixed with 1.43% ($\Gamma_1 = 0.6$, $c_c^{max} = 0.117$). [Color figure can be viewed at wileyonlinelibrary.com]

becomes a 0D problem. This could be observed according to the following rule

$$\lim_{\Gamma_1^A \to 0+} \frac{1}{\Gamma_1^A \left(c_c^{max} - c_c^{ini}\right)} \left(\frac{c_c^{max} - c_c}{c_c^{max} - c_c^{ini}}\right)^{\frac{1}{\Gamma_1^A}-1} = \delta\left(c_c^{ini} - c_c\right) \quad (43)$$

for $c_c^{ini} \le c_c$, which could lead to

$$\lim_{\Gamma_{1,bm} \to 0+} p_1^F(c_c) = \int_{c_c^{min}}^{c_c} \delta\left(c_c^{ini} - c_c\right) p_1^S\left(c_c^{ini}\right) dc_c^{ini} = p_1^S(c_c) \quad (44)$$

$$\lim_{\Gamma_{1,bm} \to 0+} p_1^S(c_c) = \int_{c_c^{min}}^{c_c} \delta\left(c_c^{ini} - c_c\right) p_1^F\left(c_c^{ini}\right) dc_c^{ini} = p_1^F(c_c) \quad (45)$$

Another extreme condition, i.e., $\Gamma_{1,\,bm} \to +\infty$ or $F_{bm} = 0$, means the two connected beds have no back mixing flow.

Figures 8 and 9 show the simulated PDFs of coke content of two reactor–regenerator systems where the average coke contents of two regenerators are fixed with 1.43%. In Figure 8, with $\Gamma_1 = 0.6$, the PDFs of coke content of the regenerator are almost identical when $\frac{\Gamma_{1,bm}}{\Gamma_1}$ ranges from 0.01 to 100. However, the profiles of $p_1^F(c_c)$ and $p_1^S(c_c)$ vary with $\frac{\Gamma_{1,bm}}{\Gamma_1}$. When $\frac{\Gamma_{1,bm}}{\Gamma_1} = 0.01$, the whole catalyst particles in the reactor could be regarded as perfectly mixed, and the curves of $p_1^F(c_c)$ and $p_1^S(c_c)$ coincide. With the increasing of ratio of $\Gamma_{1,\,bm}$ to Γ_1, the coke distribution of the first bed in the reactor moves toward the lower coke content, and the distribution of the second bed moves toward the higher coke content. When the ratio of $\Gamma_{1,\,bm}$ to Γ_1 larger than 10, both $p_1^F(c_c)$ and $p_1^S(c_c)$ are nearly convergent, which means the back mixing flow of catalyst particles between two beds could be neglected. The situation with Γ_1 = 3.0 is shown in Figure 9. However, there exists a distinct difference between them. For Γ_1 = 0.6, the coke distributions of both beds in the reactor narrows with increasing of the ratio of $\Gamma_{1,\,bm}$ to Γ_1, as shown in Figure 8. While for Γ_1 = 3.0, the change of the profile shape of coke distributions of two beds is relatively not obvious.

Simulations of MTO reactor–regenerator systems

The effect of the coke distribution on the real reactor–regenerator systems was investigated in this section. Table 1 gives the parameters and operation conditions of three MTO reactors of different scale, and the geometries of these reactors are given in Supporting Information Appendix D. In our simulation model, the diameter of each reactor is assumed to be uniform, which is same with that of its dense phase part (above the distributor). That is to say, the modeling pilot-scale reactor assumed to have a uniform diameter of 0.261 m, the

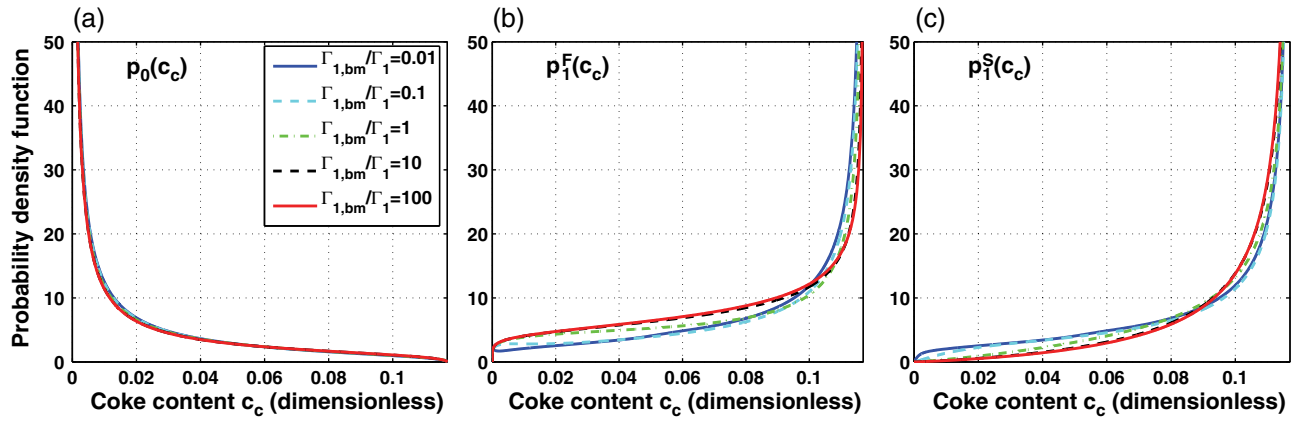

Figure 9. The coke distributions of reactor–regenerator system. (a) $p_0(c_c)$, (b) $p_1^F(c_c)$, and (c) $p_1^S(c_c)$.

The average coke content of the regenerator is fixed with 1.43% ($\Gamma_1 = 3.0$, $c_c^{max} = 0.117$). [Color figure can be viewed at wileyonlinelibrary.com]

Table 1. The Operation Conditions of MTO Reactors of Different Size

Parameters*	Pilot-scale	Demo-scale	Commercial-scale
$m^{\text{inlet}}_{\text{MeOH}}$ ($\frac{\text{kg}}{\text{h}}$)	18	2032	241,000
$m^{\text{inlet}}_{\text{H}_2\text{O}}$ ($\frac{\text{kg}}{\text{h}}$)	4.5	610	60,250
F ($\frac{\text{kg}}{\text{h}}$)	4–8.8[†]	351[†]	42,000[§]
W_1 (kg)	9	501	56,000
T (°C)	466	500	475
P (MPa)	0.024	0.103	0.108
d (m)	0.261	1.25	10.5
h (m)	2.7	6.62	26.2

*Here, m_i^{inlet} denotes the inlet amount of species i, T represents the temperature, P is the gage pressure, d the simplified diameter, and h the simplified height of the reactor.
[†]The catalyst particles of inflow have zero coke content.
[§]The catalyst particles of inflow have average coke content of 1.43%.

demonstration-scale reactor assumed to have diameter of 1.25 m, and the commercial-scale reactor of 10.5 m. The simulations combined the coke distribution model, MTO kinetic model, and GFBR model (see section *Application to MTO Process* for details). The parameter Γ_1 is defined as the product of average residence time and coke deposition rate, which is actually the Damkohler number. The average residence time τ for each reactor was predicted by the ratio of the catalyst inventory W to catalyst flux F, i.e., $\tau = W/F$. For all three scales of reactors, the catalyst inventory W can be directly measured based on pressure drop of the dense bed. The catalyst flux F for both the pilot plant and demonstration unit can be obtained according to the readings of the catalyst circulation rate that is carefully calibrated before the experiments. For commercial unit, the catalyst circulation rate is obtained via the heat balance calculation in the MTO fluidized bed regenerator. The rate constant of coke deposition k_d is calculated by iteration, which is described at the last paragraph of section *Reactor Model*.

Note that the coke distribution model was developed based on mass balance, in principle it could be considered as a generic model that can be used in a wide range. In real application, however, it replies essentially on the coke deposition rate and burning rate. MTO is a quite involved process with complicated reaction network. As mentioned above, both the coke deposition rate and burning rate were obtained based on experiments carried out at laboratory-scale MTO fluidized bed setups. The operation conditions of these experiments were carefully chosen to cover the range of industrial operation conditions. Even though, however, we would stress that the rate data should be used with caution for operating conditions beyond the experiments. Particularly the space velocity and catalyst residence time have pronounced impact on the coke deposition rate, and the used coke deposition rate works well for WHSV in the range of 1.5–5.20 $\frac{\text{kg MeOH}}{\text{kg Cat h}}$ and catalyst residence time not exceeding 3 h.

For the pilot-scale reactor, the effect of residence time on the product selectivity was investigated by keeping catalyst inventory of 9 kg and changing the catalyst inflow from 4 to 8.8 $\frac{\text{kg}}{\text{h}}$. By solving control equations of the reactor that based on the proposed coke equations, the relation of Γ_1 ($\Gamma_1 \equiv \tau_1 k_d$) and k_d with the average residence time could be predicted, as shown in Figure 10. Both Γ_1 and k_d are monotonically increasing functions. It could be seen that the variation of deposition constant k_d is small, which only ranges from 0.95 to 0.98 $\frac{1}{\text{h}}$ when the range of average residence time between 1.02 and

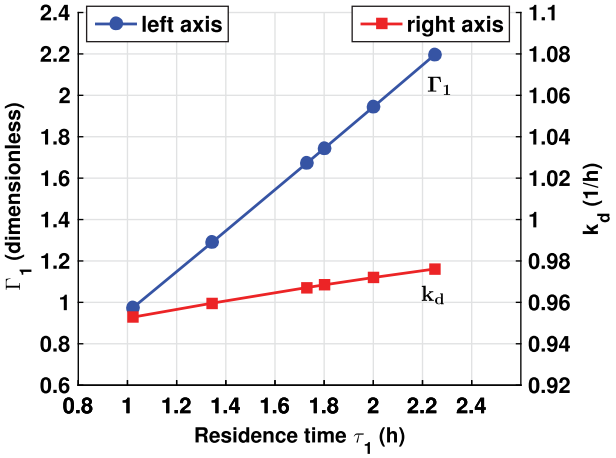

Figure 10. The simulated Γ_1 and k_d as a function of residence time of pilot-scale reactor.
[Color figure can be viewed at wileyonlinelibrary.com]

2.25 h. The profiles of corresponding coke distributions could be estimated from Figure 3 by the predicted values of Γ_1.

Meanwhile, the simulated results of product selectivity and methanol conversion also could be obtained, as shown in Figure 11. It represents a feature of the effect of the coke distribution: though the corresponding average coke content $\overline{c_{c1}}$ ranges from 5.66% to 7.88% (Figure 12), the variations of product selectivity are very small (Figure 11), which is far different from that of fixed fluidized bed (see reference [5] for detail). The difference arises from coke distribution of reactor–regenerator system and deactivation function $\phi(c_c)$ of catalyst. The product selectivity of a fixed fluidized bed is dependent upon the coke content on catalyst particles, while the selectivity of a reactor–regenerator system is determined by both two items, i.e., $\overline{(c_c\phi)}_1$ and $\overline{(s\phi)}_1$, where the coke distribution, combined with deactivation function, plays an important role. For a fixed fluidized bed, coke content c_c, based on dual-cycle mechanism, could represent the weight of importance of aromatic-based cycle, and active site content $s(c_c)$, i.e., $c_c^{\max} - c_c$, could represent the weight of importance of olefin-based cycle. However, for a reactor-regenerator system

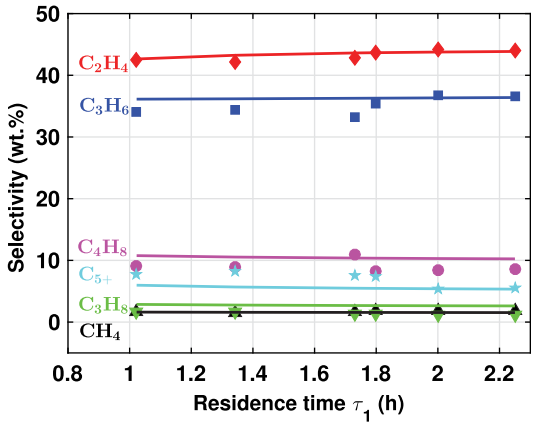

Figure 11. The simulated selectivity compared with experiment values.
The simulated values are plotted by solid lines, and the experimental values are shown by discrete markers. The simulated conversions of methanol and experimental values are all close to 100%. [Color figure can be viewed at wileyonlinelibrary.com]

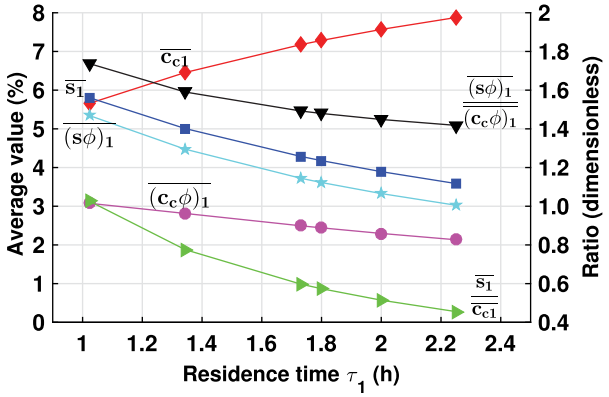

Figure 12. The simulated $\overline{c_{c1}}$, $\overline{s_1}$, $\overline{(c_c\phi)_1}$ and $\overline{(s\phi)_1}$ as a function of average residence time (left axis). The ratio of $\overline{s_1}$ to $\overline{c_{c1}}$, and the ratio of $\overline{(s\phi)_1}$ to $\overline{(c_c\phi)_1}$ are shown with right axis.

[Color figure can be viewed at wileyonlinelibrary.com]

$\overline{(c_c\phi)_1}$ and $\overline{(s\phi)_1}$, not $\overline{c_{c1}}$ and $\overline{s_1}$, represent the weights of aromatic-based cycle and olefin-based cycle, respectively. These two terms could reveal the lower activity of catalyst particles if the coke accumulates to a certain amount. It could be found that the profile of $\overline{(c_c\phi)_1}$ is different with that of $\overline{c_{c1}}$, because more coke content are grown into inactivity region with the increasing of average residence time (within our experiment range). Approximately, the quantity $\overline{(s\phi)_1}/\overline{(c_c\phi)_1}$ could be used to represent the weight of two reaction cycles of the reactor, as well as the product selectivity, while $s(c_c)/c_c$ may indicate that of fixed fluidized bed. From Figure 12, it could see that the variation of $\overline{(s\phi)_1}/\overline{(c_c\phi)_1}$ is more gentler than $\overline{s_1}/\overline{c_{c1}}$, which may interpret the small variation of product selectivity.

Based on the pilot-scale condition given at Table 1, we also could model the behavior for $\tau_1 = 0.01$–1 by increasing the catalyst flux F. The simulation results were given in Figure 13. The decreasing of residence time of catalyst particles could reduce the catalyst coke content and Γ_1. And the small Γ_1 means that the catalyst particles with small coke content dominate in the reactor, as shown in Figure 3. For catalyst particles with small coke content, the deactivation function

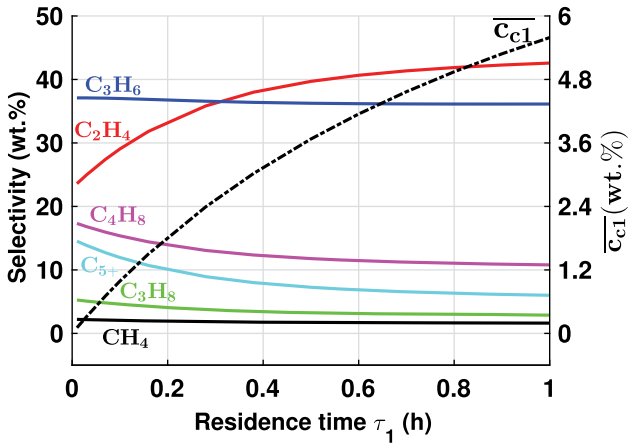

Figure 13. The simulated selectivity (left axis) and average coke content (right axis).

The simulated conversions of methanol are close to 100%. [Color figure can be viewed at wileyonlinelibrary.com]

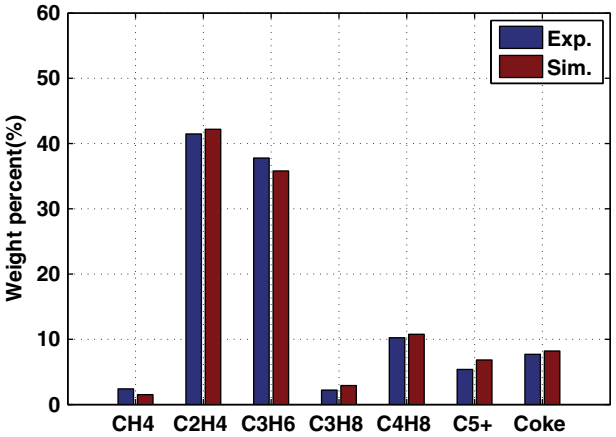

Figure 14. The comparison of the simulated selectivity of products and average coke content with the operation data of a 16 kt/a demonstration DMTO unit.

The simulated conversion of methanol is 99.97%, and the corresponding operation data is 99.97%. [Color figure can be viewed at wileyonlinelibrary.com]

$\phi(c_c)$ have value close to 1, and has little effect on reaction. Therefore, in Figure 13, the product selectivity over average coke content shows a similarity of that in a fixed bed reactor, when the residence time is small.

For demonstration-scale reactor, the product selectivity and methanol conversion were calculated based on control equations and coke distribution equations. Figure 14 shows the comparison of simulated results and the corresponding operation data. The simulated values are in agreement with the corresponding operation data. The WHSV of the reactor is 4.1 $\frac{\text{kg MeOH}}{\text{kg Cat h}}$, and the average residence time is 1.43 h. The operation condition falls in the range of the experiments by which the kinetic parameters were fitted. Since in this reactor where the inflow catalyst particles have zero coke content, the Γ_1 is the only factor that determines the coke distribution. The simulated Γ_1 of the demonstration reactor is 1.91, which means that a large portion of catalyst particles have high coke content, as shown in Figure 3. The simulated average coke content is 8.20%, which is close to the experimental result of 7.7%. And the predicted $\overline{(c_c\phi)_1}$ is about 1.21%, which is much smaller than the average coke content, indicating that many catalyst particles fall in the deactivation region. However, the amount of active catalyst particles are still sufficient to fully convert the methanol feed, thus the methanol conversion is nearly 100%, which is close to the experimental results.

For commercial-scale reactor, the product selectivity and methanol conversion were also calculated based on the same equations. However, the inflow catalyst particles, different with other two reactors, have a nonzero coke content. Then $p_1(c_c)$ and $p_0(c_c)$ should be calculated simultaneously, as described in last section, to obtain the correct results of steady-state of the reactor–regenerator system. The solving procedure is similar with that shown in Figure 6. When the whole reactor–regenerator system reaches balance, Γ_1 was found to have a value of 1.80. It also indicates that most catalyst particles, similar with demonstration-scale reactor, have high coke content. The simulated average coke content is 8.07%, which is also close to the experimental value of 7.95%. The $\overline{(s\phi)_1}$ and $\overline{(c_c\phi)_1}$ are predicted with 2.40 and

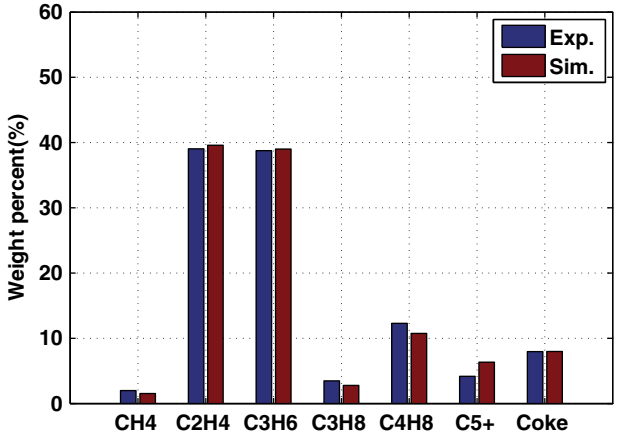

Figure 15. The comparison of the simulated selectivity of products and average coke content with the operation data of a 1.8 MMt/a industrial DMTO unit.

The simulated conversion of methanol is 100.00%, and the corresponding operation data is 99.92%. [Color figure can be viewed at wileyonlinelibrary.com]

1.25%, respectively. The simulated product selectivity are in good agreement with the corresponding experiment values, as shown in Figure 15. The simulated conversion of methanol is 100.00%, which is close to the experiment value 99.92% too.

In MTO reaction over SAPO-34 catalyst, due to high activity of methanol, the methanol can easily be fully converted. Thus, in all experiments reported in this article, the conversion of methanol was almost 100%, which is consistent with our simulation results for pilot plant, demonstration, and commercial units. In fact within the application range of the rate constants in our kinetic model, the change of Γ_1 only has a minor impact on the conversion of methanol. For example, for pilot plant scale reactor, the variation of Γ_1 from 1 to 2.2 shows a negligible change of the conversion of methanol.

However, the product selectivity is dependent upon the coke distribution, thus sensitive to Damkohler number Γ_1. If the inflow catalyst particles have no or negligibly small coke content, the coke distribution for different Γ_1 is shown in Figure 3. From Figure 3, it can be found that for Γ_1 smaller than 1 catalyst particles with light coke deposition dominates; while as Γ_1 becomes larger than 1, catalyst particles with heavy coke deposition dominates. The slope of coke distribution function varies more rapid when Γ_1 is larger than 1. This means that for $\Gamma_1 > 1$ on average the catalyst particles accumulate more coke, which can, on the one hand, prompt product selectivity and, on the other hand, accelerate the deactivation of catalyst particles. The findings in Figure 3 can confirm the results in Figures 11 and 13, in which we show the change of product selectivity with residence time in pilot-scale reactor as the deposition constant k_d is almost constant in the reactor. As can be seen, the variation of product selectivity becomes more pronounced when Γ_1 reduces from larger than 1 to smaller than 1 in pilot-scale reactor, which is consistent with the results in Figure 3.

Coke distribution in scaling up the fluidized bed reactor

For most of catalytic processes including MTO and FCC, the decay of activity of catalyst is directly related to the deposition of coke on catalyst particles. In other words, the coke content on any catalyst particle can, to a large extend, denote its activity in these processes, which determines the product selectivity and reactant conversion. Suppose that (a) the catalyst particles in a fluidized bed are ideally mixed, and (b) the mass transfer between gas and catalyst particle impose only a minor impact on the reaction, the coke distribution is in principle the dominant factor determining the product selectivity and reactant conversion. That is, the same coke distribution will lead to similar product selectivity and reactant conversion. In this connection, we argue that the coke distribution can be used to scale up the catalytic fluidized bed reactor. Since the Damkohler number Γ_1 plays a key role for determining the coke distribution when the initial coke content of the inflow catalyst particles is sufficiently small, it may be used as the key parameter for scaling up the fluidized bed reactor.

In MTO process, the mass transfer between gas and catalyst has a relatively small impact on the reaction rate, thus, it is possible to use the coke distribution to scale up the MTO fluidized bed reactor. In doing so, it is essentially to keep the Damkohler number Γ_1 constant for MTO fluidized bed reactors at different scales. As shown above, our model can predict the experimental results at various scales. We further analyze the Damkohler number Γ_1 for MTO reactors at different scales. From Figure 10, it can be found that Γ_1 for the pilot-scale reactor is in the range of 1.0–2.2, and the Γ_1 for an optimal selectivity is around 2.0. For the demonstration reactor, a relatively optimal product selectivity was obtained under the operational condition as given in Table 1. The corresponding Γ_1 is 1.91, and the catalyst particles with high coke content dominate according to the shape of the coke distribution as shown in Figure 3. For the commercial-scale reactor, a relatively optimal product selectivity was obtained with Γ_1 of 1.80 whereas the inflow catalyst particles has a small coke content of 1.43%. The consistence of the Damkohler number Γ_1 for MTO fluidized bed reactors at all three scales based on the post prior analysis further confirms the role of the Damkohler number Γ_1 in scaling up of MTO fluidized bed reactor.

If the mass transfer between gas and catalyst particles possesses constraints, the Damkohler number Γ_1 may not be the only dominant parameter for scaling up the catalytic fluidized bed reactor. In this case, the effect of gas–solid mass transfer on scaling up needs to be considered, which in turns necessitates the study of hydrodynamics of gas–solid two-phase flows in fluidized beds. In this regard, either the simple GFBR model or sophisticated CFD model, if validated by experiments, can be used.

Conclusions

In this work, a coke distribution model for catalyst particles in fluidized bed was developed based on population balance or mass balance theory. A 3D time-dependent partial differential equation, as well as some simplified equations, is proposed to describe the PDF of coke content on catalyst particles. An analytic solution of coke distribution for 0D time-independent problem is provided. And this solution is extended for solving nonzero-dimensional time-independent problem.

For 0D time-independent problem, the coke distribution of catalyst particle is dependent upon three factors, i.e., average catalyst residence time, coke deposition (or burning) rate, and coke distribution of catalyst inflow. For coke deposition rate linearly dependent on coke content, the first two factors could be considered together as a dimensionless number. Such as for MTO process, these first two factors, based on our proposed kinetics,[5] are ascribed to the Dahmkohler number Γ_1 ($\Gamma_1 \equiv$

$\tau_1 k_d$). When the inflow of catalyst particles has a single coke content, Γ_1 determines the PDF shape of the coke distribution: it is monotonically decreasing if $\Gamma_1 < 1$, monotonically increasing if $\Gamma_1 > 1$, and constant for $\Gamma_1 = 1$. When the inflow of catalyst particles has a wide distribution of coke content, the effect of Γ_1 on the shape of the PDF is more complex. According to our simulations of a reactor–regenerator system, it seems that $\Gamma_1 = 1$ also becomes a critical point for the profile of the PDF of coke content.

Research on the coke distribution is of great importance for the system where coke plays an important role in reaction rate. Such as for MTO process, the coke content determines the product selectivity and affects methanol conversion. Therefore, the experience obtained from a fixed fluidized bed cannot be directly applied to a reactor–regenerator system. For MTO reactor–regenerator system, the effect of coke distribution could be represented by two parameters, i.e., $\overline{(s\phi)}_1$ and $\overline{(c_c\phi)}_1$, which is different from fixed fluidized bed. We had simulated three scales of MTO reactors, by combining the coke distribution model, MTO kinetic model and GFBR model. All simulated results were in good agreement with the experimental data. This shows that the coke distribution model can be potentially used to optimize the MTO fluidized bed reactor design and operation. It may also be used for scaling up some catalytic processes where the coke contents is decisive to product selectivity and reactant conversion.

Acknowledgment

This work is supported by the National Natural Science Foundation of China (Grant No. 91834302).

Notation

c_c coke content of catalyst particles, *dimensionless*
c_c^0 single coke content of inflow catalyst particles, *dimensionless*
c_c^{min} minimum coke content of catalyst particles, *dimensionless*
c_c^{max} maximum coke content of catalyst particles, *dimensionless*
$\vec{x}$ spacial location of a catalyst particle, m
t time, s
τ average residence time of catalyst particles in the fluidized bed, s
τ^P average residence time of catalyst particles of cell P, s
$R(c_c)$ rate of coke deposition or burning (a function of coke content), $\frac{1}{s}$
$\vec{v}$ spacial velocity of a catalyst particle, $\frac{m}{s}$
$p(\vec{x}, c_c, t)$ coke content PDF (probability density function) of catalyst particles in the bed (a function of spacial location, coke content and time), *dimensionless*
$p(c_c, t)$ coke content PDF of catalyst particles in the bed (a function of coke content and time), *dimensionless*
$p(c_c)$ coke content PDF of catalyst particles in the bed (a function of coke content), *dimensionless*
$p_{in}(c_c, t)$ coke content PDF of inflow catalyst particles (a function of coke content and time), *dimensionless*
$p_{in}(c_c)$ coke content PDF of inflow catalyst particles (a function of coke content), *dimensionless*
$p^P(c_c)$ coke content PDF of cell P (a function of coke content), *dimensionless*
$p^{N_f}(c_c)$ coke content PDF of the neighbor cell that connected cell P by face f (a function of coke content), *dimensionless*
$E(t)$ residence time distribution function, $\frac{1}{s}$
$\rho_{cat}(\vec{x}, t)$ time-dependent mass density of catalyst particles at location $\vec{x}$ and time t, $\frac{kg}{m^3}$
$W(t)$ catalyst inventory in the bed (a function of time), kg
W catalyst inventory in the bed, kg
$F_{in}(t)$ inflow flux of catalyst particles (a function of time), $\frac{kg}{s}$
$F_{out}(t)$ outflow flux of catalyst particles (a function of time), $\frac{kg}{s}$
F catalyst flux of the bed, $\frac{kg}{s}$
F^f catalyst influx through face f of cell P, $\frac{kg}{s}$
F^P catalyst influx or outflow of cell P, $\frac{kg}{s}$
z coordinate of reactor axis (z-axis), m
v_z catalyst velocity along reactor axis (z-axis), $\frac{m}{s}$
$s(c_c)$ active site content of the catalyst particle, i.e., $c_c^{max} - c_c$, *dimensionless*
k_d rate constant of coke deposition, $\frac{1}{s}$
k_b rate constant of coke burning, $\frac{1}{s}$
ψ phase volume fraction, *dimensionless*
u superficial velocity of gas, $\frac{m}{s}$
D axial gas dispersion coefficient, $\frac{m^2}{s}$
C_i concentration of species i, $\frac{kmol}{m^3}$
r_i reaction rate of species i, $\frac{kmol}{m^3 s}$
k_{LH} gas interchange coefficient between L and H phases, $\frac{m}{s}$
a_I interphase transfer surface (m^2) per unit volume (m^3) of gas in low-density phase, $\frac{m^2 \text{ interface}}{m^3 \text{ gas in low density phase}}$
c_{ji} coefficient of species i of reaction equation j, *dimensionless*
M_i molar mass of species i, $\frac{kg}{kmol}$
$\mathcal{R}_j(c_c)$ reaction rate of reaction equation j, $\frac{kg}{m^3 s}$
ϵ voidage of the phase, *dimensionless*
k_j^e effective rate parameter of equation j, $\frac{kg}{m^3 s}$
$\phi(c_c)$ deactivation function of catalyst particles, *dimensionless*
c_c^{cri} activation parameter of catalyst particles, *dimensionless*
WHSV the ratio of the methanol influx to the mass of catalyst particles in the reactor, $\frac{kg\ MeOH}{kg\ Cat\ h}$
Γ_1 Damkohler number, i.e., $\tau_1 k_d$, *dimensionless*

Subscripts and Superscripts

− mean value
0 regenerator ($p(c_c)$, W, τ, c_c, $R(c_c)$)
1 reactor ($p(c_c)$, W, τ, c_c, $R(c_c)$)
L low-density phase
H high-density phase
f freeboard
F first bed
S second bed
bm back maxing catalyst particles

Literature Cited

1. Froment GF. Kinetic modeling of hydrocarbon processing and the effect of catalyst deactivation by coke formation. *Catal Rev*. 2008; 50(1):1-18.
2. Berrouk AS, Pornsilph C, Bale SS, Du Y, Nandakumar K. Simulation of a large-scale FCC riser using a combination of MP-PIC and four-lump oil-cracking kinetic models. *Energy Fuel*. 2017;31(5):4758-4770.
3. Alwahabi SM, Froment GF. Single event kinetic modeling of the methanol-to-olefins process on SAPO-34. *Ind Eng Chem Res*. 2004; 43(17):5098-5111.
4. Ying L, Yuan X, Ye M, Cheng Y, Li X, Liu Z. A seven lumped kinetic model for industrial catalyst in DMTO process. *Chem Eng Res Des*. 2015;100:179-191.
5. Yuan X, Li H, Ye M, Liu Z. Kinetic modeling of methanol to olefins process over SAPO-34 catalyst based on the dual-cycle mechanism. *AIChE J*. 2018. http://doi.org/10.1002/aic.16439
6. Bos ANR, Tromp PJJ, Akse HN. Conversion of methanol to lower olefins. Kinetic modeling, reactor simulation, and selection. *Ind Eng Chem Res*. 1995;34(11):3808-3816.
7. Zheng K, Cheng Y, Li X. Simulation of fluidized bed reactor for methanol to olefins (MTO) process. *J Chem Eng Chin Univ*. 2012;(01): 69-76.
8. Hulburt H, Katz S. Some problems in particle technology: A statistical mechanical formulation. *Chem Eng Sci*. 1964;19(8):555-574.
9. Levenspiel O, Kunii D, Fitzgerald T. The processing of solids of changing size in bubbling fluidized beds. *Powder Technol*. 1968;2(2): 87-96.
10. Tian P, Wei Y, Ye M, Liu Z. Methanol to olefins (MTO): from fundamentals to commercialization. *ACS Catal*. 2015;5(3):1922-1938.

11. Ye M, Li H, Zhao Y, Zhang T, Liu Z. Chapter five - MTO processes development: the key of mesoscale studies. *Adv Chem Eng*. 2015;47:279-335.
12. Liu Z, Liu Y, Ye M, Qiao L, Shi L, Ma X. Process technology for DMTO unit with a capacity of 1.8 MM TPY methanol feed and unit features. *Petrol Refinery Eng*. 2014;44(7):1-6.
13. Soundararajan S, Dalai A, Berruti F. Modeling of methanol to olefins (MTO) process in a circulating fluidized bed reactor. *Fuel*. 2001;80(8): 1187-1197.
14. Chang J, Zhang K, Chen H, Yang Y, Zhang L. CFD modelling of the hydrodynamics and kinetic reactions in a fluidised-bed MTO reactor. *Chem Eng Res Des*. 2013;91(12):2355-2368.
15. Lu B, Luo H, Li H, et al. Speeding up CFD simulation of fluidized bed reactor for MTO by coupling CRE model. *Chem Eng Sci*. 2016; 143:341-350.
16. Zhu LT, Pan H, Su YH, Luo ZH. Effect of particle polydispersity on flow and reaction behaviors of methanol-to-olefins fluidized bed reactors. *Ind Eng Chem Res*. 2017;56(4):1090-1102.
17. Abba IA, Grace JR, Bi HT, Thompson ML. Spanning the flow regimes: generic fluidized-bed reactor model. *AIChE J*. 2003;49(7): 1838-1848.

Manuscript received Mar. 29, 2018, and revision received Nov. 9, 2018.